Modeling and Analysis of Eddy-Current Damping for High-Precision Magnetic Levitation of a Small Magnet

Caglar Elbuken, Ehsan Shameli, and Mir Behrad Khamesee

Department of Mechanical Engineering, University of Waterloo, Waterloo, ON N2L3G1, Canada

This paper presents modeling and analysis of eddy-current damping that is formed by a conductive plate placed below the levitating object in order to suppress vibrations and ensure stability. It is demonstrated that vibrations should be damped to preserve stability and precision especially for stepwise motion. The levitated object is a small permanent magnet in our experiments. A magnetic drive unit is used for vertical motion of the magnet. Eddy-current distribution in the plate is calculated by solving diffusion equation for vector magnetic potential. The eddy force applied to the object is derived by a coil model representation. It is shown that if a 20 mm radius, 9 mm thick aluminum circular plate is used for eddy-current damping, the levitated object can closely follow a step input with a steady-state precision varying between 0.04 and 0.07 mm depending on the plate object distance. Eddy-current damping is a key technique that improves levitation performance to increase the diversity of applications of magnetic levitation systems in micromanipulation and microelectronic fabrication.

Index Terms—**Eddy current, eddy-current damping, magnetic levitation, mechatronics, modeling.**

I. Introduction

MAGNETIC levitation is a promising technology for noncontact manipulation of objects using magnetic field. Since long-reached and jointed parts are not used, wear and maintenance problems caused by friction are eliminated. Magnetic levitation has uses in teleoperation [1]–[3], magnetic bearings [4], [5], conveyors [6], microassembly [7], [8], and microelectronic fabrication [9]–[11].

In most of these applications, precision of levitated motion and fast dynamic response are the two main requirements. In our previous studies [12], [13]; it was shown that the system response to a ramp input is satisfactory, meaning that the levitated object could closely follow a ramp reference input. However, when a step input was applied, the object experienced a high over/under-shoot [2], [9], [13]. This behavior is undesirable for high-precision applications. The system can even become unstable, if a higher amplitude step input is applied. Such a response is mainly because the controller and environment dampings are not enough. To obtain a more robust and precise magnetic levitation, an eddy-current damping method is proposed in this paper.

Recently, Sodano and Bae [14] discussed various uses of eddy-current damping in many areas. They emphasized that principal effects of eddy-current damping are suppression of vibration and magnetic braking. Eddy-current damping is successfully applied to damp vibrations in many devices such as rotors [15], [16], satellites [17], spacecraft solar arrays [18], and microfabrication tools [19], [20] to increase precision.

Although Teshima *et al.* [21] and Park *et al.* [9] used eddy-current damping for superconducting levitation and magnetic levitation, respectively, they based their damping discussion on experimental work. However, determining the forces affecting the levitating object is crucial for teleoperation and microassembly. Calculating the eddy damping force allows for a better understanding of magnetic levitation which therefore leads to improved controller designs and higher precisions.

In this study, by placing a conductive plate underneath the levitated object, eddy-current damping was introduced to suppress vibrations and to ensure stability of magnetic levitation for high-amplitude step inputs. Eddy-current generation is modeled and a method is provided to calculate the damping eddy force. Following the comparison of theory and experimental results, step transient motion of levitation with eddy-current damping is presented.

II. Magnetic Levitation System

A magnetic levitation setup was constructed which consists of a controller, a CCD laser line displacement sensor, an iron yoke, and seven identical electromagnets connected with a pole piece. Each electromagnet has a magnetomotive force of 1543 ampere-turns with 750 turns of wire and a current limit of slightly greater than 2A. Only vertical motion of the object is examined, so the laser sensor measures $\hat{z}$ axis position at every 5 ms. The origin is taken to be the center of the pole piece. At every 5 ms, the state feedback controller calculates the current to be applied to the electromagnets depending on the position of the levitated object. A 40 V power supply is used to obtain the required current levels so that position of the object is readjusted by time-varying levitation force. The computer communicates through 16-bit A/D and 16-bit D/A converters with operating ranges of ± 5 V and ± 10 V. A schematic diagram and photograph of the system are shown in Figs. 1 and 2, respectively.

The laser sensor is a Keyence LS-5000, 0.2–40 mm measuring range with a maximum resolution of 0.05 μm which results in a position error of approximately 16 μm because of

Digital Object Identifier 10.1109/TMAG.2006.885859

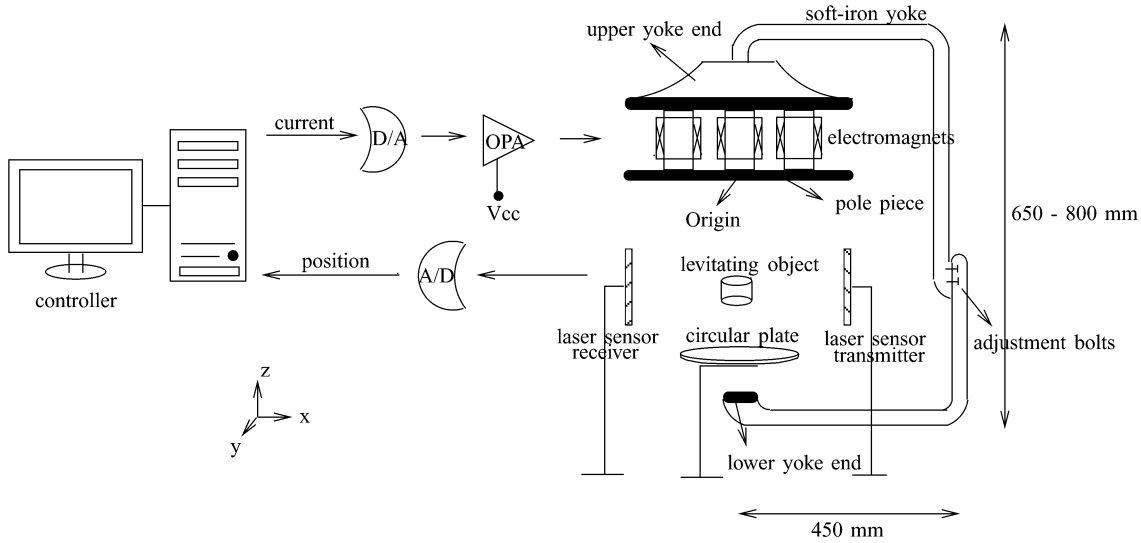

Fig. 1. Schematic of magnetic levitation system.

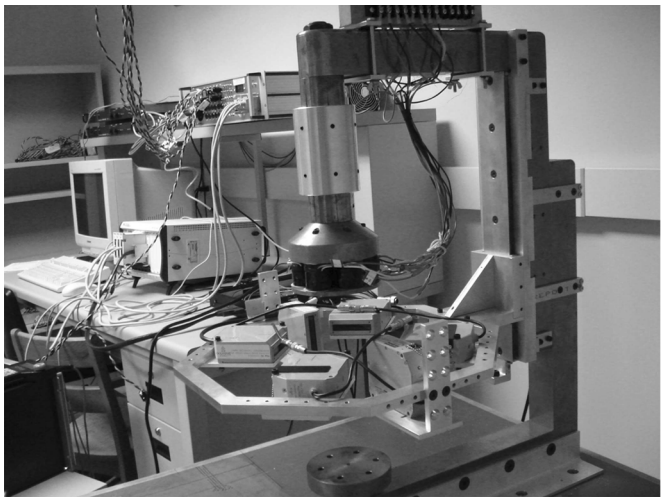

Fig. 2. Picture of the levitation system.

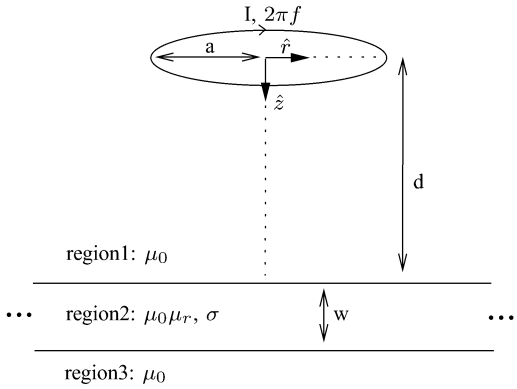

Fig. 3. The coil model.

the hardware noise and data conversions. The levitated object is a 5 mm radius, 10 mm height cylindrical NdFeB permanent magnet with a magnetic dipole moment of 0.785 Am^2 in $+\hat{z}$ direction. The levitated magnet has a mass of 6.59 g.

III. Eddy-Current Modeling

To introduce eddy-current damping to the levitation system, a circular aluminum plate is used. The 6061 aluminum plate is placed on a glass stand, below the working domain of the magnet (Fig. 1).

Changing magnetic field forms circulating eddy currents in the plate. The direction of this current is such that, magnetic field generated by these eddy currents oppose the change in the field itself. In our system, the change in the magnetic field is caused by the time varying magnetic field of electromagnets and the magnetic field of the object. When the object vibrates during levitation, flux passing through the plate changes because of the changing electromagnet currents and the varying field of the object. Consequently, circulating eddy currents are induced and a damping force is applied to the object.

In this section, the formulas for eddy-current distribution and the resultant eddy force are derived using a simplified model. The changing magnetic field is taken to be generated by an alternating current carrying wire. The wire is placed horizontally with its center at the origin (Fig. 3). There is a conductive plate at a distance of d from the wire. For simplicity, the plate is assumed to be infinite extent in horizontal plane. It has a thickness of w, relative permeability of μ_r, and conductivity of σ.

It is well known that for such a setup, time-varying current passing through the wire forms changing magnetic field. This generates an electric field, which forms the eddy currents in the plate (region-2). Starting with the fundamental equations

$$\nabla \times \mathbf{E} = -\frac{\partial \mathbf{B}}{\partial t} \tag{1}$$

$$\mathbf{J} = \sigma \mathbf{E} \tag{2}$$

curl of current density is obtained as

$$\nabla \times \mathbf{J} = -\sigma \frac{\partial \mathbf{B}}{\partial t} \tag{3}$$

where E [V/m] is the electric field, J [A/m^2] is the current density and B [T] is the magnetic flux density (we will call magnetic field). Expressing magnetic field as the curl of vector magnetic potential, $\mathbf{B} = \nabla \times \mathbf{A}$, the current density is written as

$$\mathbf{J} = -\sigma \frac{\partial \mathbf{A}}{\partial t}. \tag{4}$$

Using Ampere's law, $\nabla \times \mathbf{B} = \mu \mathbf{J}$, diffusion equation for vector magnetic potential is found to be

$$\nabla^2 \mathbf{A} = \mu\sigma \frac{\partial \mathbf{A}}{\partial t}. \tag{5}$$

Equation (5), for three regions in Fig. 3 can be written as [22]

$$\nabla^2 \mathbf{A}_{1,\varphi} = 0 \tag{6}$$
$$\nabla^2 \mathbf{A}_{2,\varphi} = j2\pi f \mu\sigma \mathbf{A}_{2,\varphi} \tag{7}$$
$$\nabla^2 \mathbf{A}_{3,\varphi} = 0 \tag{8}$$

where $A_{i,\varphi}$ denotes the φ component of vector magnetic potential in region i and f denotes the frequency of the current in the wire. Vector magnetic potential has only φ component since current is varying with φ.

The solution of diffusion (5) for cylindrical coordinate system can be obtained by the method of separation of variables. The general solution of (6)–(8) is given as follows [23]:

$$\mathbf{A}_{1,\varphi} = \mu_0 \int_0^\infty \frac{I}{2} e^{-kz/a} J_1(k) J_1(kr/a) + L(k) e^{kz/a} J_1(kr/a) dk \tag{9}$$
$$\mathbf{A}_{2,\varphi} = \mu \int_0^\infty M(k) e^{-qz/a} J_1(kr/a) + N(k) e^{qz/a} J_1(kr/a) dk \tag{10}$$
$$\mathbf{A}_{3,\varphi} = \mu_0 \int_0^\infty P(k) e^{-kz/a} J_1(kr/a) dk \tag{11}$$

where I is the coil current phasor, a is the coil radius, J_1 is a Bessel function of the first kind, $q = \sqrt{k^2 + jp^2}$ and $p = \sqrt{\mu 2\pi f \sigma a^2}$.

Equations (9)–(11) introduce four unknown functions, $L(k)$, $M(k)$, $N(k)$, and $P(k)$. The three regions are separated by two boundaries, the top and bottom surfaces of the plate (Fig. 3). Boundary conditions for magnetic field, $\mathbf{n} \cdot (\mathbf{B_2} - \mathbf{B_1}) = 0$, and magnetic field intensity, $\mathbf{n} \times (\mathbf{H_2} - \mathbf{H_1}) = 0$, are applied at these boundaries to find the unknowns as follows:

$$M(k) = \frac{Ike^{-kd/a} J_1(k)(q + k\mu_r) e^{q(d+w)/a}}{(q + k\mu_r)^2 e^{qw/a} - (q - k\mu_r)^2 e^{-qw/a}} \tag{12}$$

$$N(k) = \frac{Ike^{-kd/a} J_1(k)(q - k\mu_r) e^{-q(d+w)/a}}{(q + k\mu_r)^2 e^{qw/a} - (q - k\mu_r)^2 e^{-qw/a}} \tag{13}$$

$$L(k) = \frac{0.5IJ_1(k)(k^2\mu_r^2 - q^2) e^{-2kd/a}(1 - e^{-2qw/a})}{(q + k\mu_r)^2 - (q - k\mu_r)^2 e^{-2qw/a}} \tag{14}$$

$$P(k) = \frac{Ike^{-kd/a} J_1(k) 2q\mu_r e^{k(d+w)/a}}{(q + k\mu_r)^2 e^{qw/a} - (q - k\mu_r)^2 e^{-qw/a}}. \tag{15}$$

Magnetic field in any region can be expressed as

$$\mathbf{B} = \nabla \times \mathbf{A} = -\hat{r} \frac{\partial A_\varphi}{\partial z} + \hat{z} \left[\frac{A_\varphi}{r} + \frac{\partial A_\varphi}{\partial r} \right]. \tag{16}$$

Substituting (12) and (13) into (10), vector magnetic potential in the plate is found to be

$$\mathbf{A}_{2,\varphi} = \mu \int_0^\infty \frac{Ike^{-kd/a} J_1(k) J_1(kr/a)(q + k\mu_r) e^{q(d+w-z)/a}}{(q+k\mu_r)^2 e^{qw/a} - (q-k\mu_r)^2 e^{-qw/a}} dk + \mu \int_0^\infty \frac{Ike^{-kd/a} J_1(k) J_1(kr/a)(q - k\mu_r) e^{-q(d+w-z)/a}}{(q+k\mu_r)^2 e^{qw/a} - (q-k\mu_r)^2 e^{-qw/a}} dk. \tag{17}$$

Consequently, the eddy-current density (4) induced in the plate takes the form

$$\mathbf{J}_{2,\varphi} = \sigma j2\pi f \mu \int_0^\infty \frac{Ike^{-kd/a} J_1(k) J_1(kr/a)(q + k\mu_r) e^{q(d+w-z)/a}}{(q-k\mu_r)^2 e^{-qw/a} - (q+k\mu_r)^2 e^{qw/a}} dk + \sigma j2\pi f \mu \int_0^\infty \frac{Ike^{-kd/a} J_1(k) J_1(kr/a)(q - k\mu_r) e^{-q(d+w-z)/a}}{(q-k\mu_r)^2 e^{-qw/a} - (q+k\mu_r)^2 e^{qw/a}} dk. \tag{18}$$

Eddy-current density in the plate is calculated for various r and z. It is observed that $\mathbf{J}_{2,\varphi} \simeq 0$ for $r \geq 20$ mm. The eddy force model developed is based on the assumption that the plate is infinite extent in horizontal plane. Therefore, the minimum plate radius is taken to be 20 mm for the experiments.

Substituting (14) into (9), vector magnetic potential for the region above the plate is obtained as

$$\mathbf{A}_{1,\varphi} = \frac{1}{2} \int_0^\infty I\mu_0 e^{-kz/a} J_1(k) J_1(kr/a) dk + \frac{1}{2} \int_0^\infty \frac{I\mu_0 J_1(k) J_1(kr/a) e^{kz/a} (k^2\mu_r^2 - q^2) e^{-2kd/a} (1 - e^{-2qw/a})}{(q + k\mu_r)^2 - (q - k\mu_r)^2 e^{-2qw/a}} dk. \tag{19}$$

Equation (19) is written as summation of two terms. The first term is the vector magnetic potential formed by the coil itself, $\mathbf{A}_{c,\varphi}$, and the second term is the vector magnetic potential generated by the eddy currents induced in the plate, $\mathbf{A}_{p,\varphi}$

$$\mathbf{A}_{1,\varphi} = \mathbf{A}_{c,\varphi} + \mathbf{A}_{p,\varphi} = \int_0^\infty U_c \, dk + \int_0^\infty U_p dk. \tag{20}$$

To investigate the effect of plate on magnetic levitation, only $\mathbf{A}_{p,\varphi}$ is used because $\mathbf{A}_{c,\varphi}$ exists independent of the plate. If

the conductive plate is used, an additional potential $(\mathbf{A}_{p,\varphi})$ is generated by induced currents. When the plate thickness decreases, $\mathbf{A}_{p,\varphi}$ also decreases converging to a limit of zero, $\lim_{w\to 0}\mathbf{A}_{p,\varphi}=0$.

Using (16), magnetic field generated by eddy currents is found to be

$$\begin{aligned}\mathbf{B}_{\text{eddy}} &= \nabla\times\mathbf{A}_{p,\varphi}\\ &= -\hat{r}\int_0^\infty \frac{k}{a}U_p dk + \hat{z}\left[\frac{\mathbf{A}_{p,\varphi}}{r}+\int_0^\infty \frac{k}{a}U_p\,dk\right]. \quad (21)\end{aligned}$$

Eddy currents form a transverse eddy force. The vertical eddy force applied to a levitating object which can be represented by a magnetic dipole moment of $\mathbf{P}=p_0\hat{z}$ can be expressed as [12]

$$\mathbf{F}=(\mathbf{P}\cdot\nabla)\mathbf{B}_{\text{eddy}} \Rightarrow F_z = p_0\frac{\partial B_{\text{eddy},z}}{\partial z}. \quad (22)$$

Substituting (21) into (22), the vertical force on the object is found for cylindrical coordinates as

$$\begin{aligned}F_z &= F_{\text{eddy}}\\ &= \hat{z}p_0\left[\frac{1}{r}\int_0^\infty \frac{k}{a}U_p\,dk+\int_0^\infty\left(\frac{k}{a}\right)^2 U_p\,dk\right] \quad (23)\end{aligned}$$

where

$$U_p = \frac{0.5I\mu_0 J_1(k)J_1(kr/a)e^{kz/a}(k^2\mu_r^2-q^2)e^{-2kd/a}(1-e^{-2qw/a})}{(q+k\mu_r)^2-(q-k\mu_r)^2e^{-2qw/a}}. \quad (24)$$

Equation (23) enables the numerical calculation of eddy force. Although integral upper limit is infinity, the force equation converges by the Bessel function, $J_1(k)$, hidden in the U_p term. Fig. 4 provides the relationship between the eddy force and the plate thickness for a certain coil and an object at the origin with $p_0=1$.[1] The plot indicates that eddy force increases up to a certain thickness and then remains constant since eddy current penetrates to a certain depth of plate.

IV. Damping Force

Eddy currents are formed by changing magnetic field. For the magnetic levitation setup shown in Fig. 1, there are two sources of the change: 1) The magnetic field of the levitated object, which is a permanent magnet. 2) The magnetic field of electromagnets that is readjusted at every 5 ms. In this section, the eddy force (F_{eddy}) applied to the object is calculated using the coil model described in the previous section.

At every 5 ms, the position of the object (z) is measured by the laser sensor and the change in position (dz/dt) is determined. Therefore, the change of the flux penetrating into the plate can be calculated. Magnetic field of the permanent magnet can be written as

$$\mathbf{B}=\frac{\mu_0}{4\pi}p_0\left(\hat{r}\frac{2\cos\theta}{r^3}+\hat{\theta}\frac{\sin\theta}{r^3}\right) \quad (25)$$

[1]To calculate force applied to an object on the central axis $(r=0)$, r should be set to a value very close to zero. The first term of (23) converges by the Bessel function inside the integral.

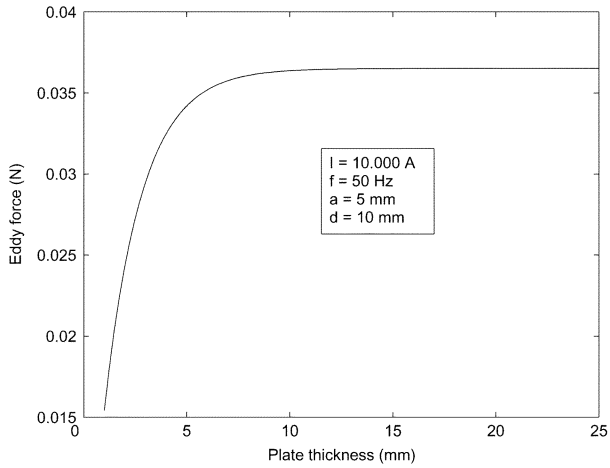

Fig. 4. Eddy force as a function of plate thickness. $\mu_{\text{plate}} = 4\pi 10^{-7}, \sigma_{\text{plate}} = 33.37\times 10^6(\text{m}\Omega)^{-1}$.

where p_0 is the dipole moment of the magnet and θ is the angle from the central axis (Fig. 5). Flux passing through the plate is equal to the flux passing through the outer surface of the semisphere shown as a dashed line in Fig. 5. Then penetrating flux can be found as

$$\begin{aligned}\Phi_{pm} &= \int \mathbf{B}\cdot d\mathbf{s} = \int_{sph}\mathbf{B}\cdot\hat{r}ds\\ &= \int_0^{cos^{-1}\frac{z}{\sqrt{z^2+b^2}}}\int_0^{2\pi} B_r r^2\sin\theta\,d\phi d\theta\\ &= \frac{\mu_0}{2}p_0\frac{b^2}{(b^2+z^2)^{3/2}}. \quad (26)\end{aligned}$$

The pm subscript in above equation denotes that the flux belongs to the permanent magnet. Change in the flux becomes

$$\frac{d\Phi_{pm}}{dt}=\frac{-3\mu_0}{2}p_0\frac{b^2 z}{(b^2+z^2)^{5/2}}\frac{dz}{dt}. \quad (27)$$

If the coil in Fig. 3 is placed above the circular plate, flux passing through the plate and its time derivative can be found in a similar way

$$\Phi_{\text{coil}}=\frac{\mu_0}{2}I\pi a^2\frac{b^2}{(b^2+d^2)^{3/2}} \quad (28)$$

$$\frac{d\Phi_{\text{coil}}}{dt}=\frac{\mu_0}{2}2\pi f I\pi a^2\frac{b^2}{(b^2+d^2)^{3/2}}. \quad (29)$$

Because of the magnetic coupling of electromagnets and the effect of pole piece, magnetic field formed by the electromagnets cannot be determined analytically. Alternatively, an experimental method was followed. By applying various currents to electromagnets, magnetic field was measured by a gaussmeter below the working domain, where the plate is located. Measurements revealed that the magnetic field [Tesla] in that area can be approximated as

$$B_{em}=\frac{2.5\times 10^{-4}}{|z|}I \quad (30)$$

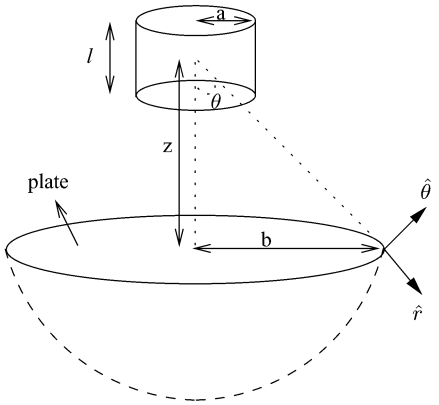

Fig. 5. Permanent magnet above a circular plate.

where I is the electromagnet current [A], $|z|$ is the distance from the electromagnets, and the em subscript denotes the electromagnets. So, flux penetrating the plate can be calculated as

$$\Phi_{em} = B_{em} \times \pi b^2 = \frac{2.5 \times 10^{-4}}{|z|} I \pi b^2. \tag{31}$$

The time derivative of flux is

$$\frac{d\Phi_{em}}{dt} = \frac{2.5 \times 10^{-4}}{|z|} \frac{dI}{dt} \pi b^2. \tag{32}$$

In Section III, eddy force is derived for a coil with four parameters, I, f, a, d. Equating the flux and its derivative for the coil [(28), (29)] to the ones for the magnet [(26), (27)] and electromagnets [(31), (32)], equivalent coils for the magnet and electromagnets can be found. Coil parameters can be written as a function of z and dz/dt, so that at anytime if z and dz/dt is known, equivalent coils that generate the same flux change can be found. Then the induced eddy current is calculated numerically using (23).

Implementing this method, the eddy force formed by the electromagnets and the permanent magnet was calculated as a function of magnet position (Fig. 6). The total eddy force was the summation of these two forces. The plate was located at $z = -0.1$ m and dz/dt was fixed to be -0.01 m/s. As expected, eddy force increased significantly when magnet approached to the plate.

V. Experimental Verification and Discussion

In order to validate the eddy force found, the vertical motion of the object was examined. Experimental and theoretical values of acceleration were compared. With the plate positioned at $z = -0.1$ m, the object was first levitated to the point of $z = -0.0932$ m and then it was moved to $z = -0.097$ m (Fig. 7). A computer recorded the position of the magnet and the currents applied to the electromagnets. Fig. 7 shows the position of the magnet and the inset shows the portion for which

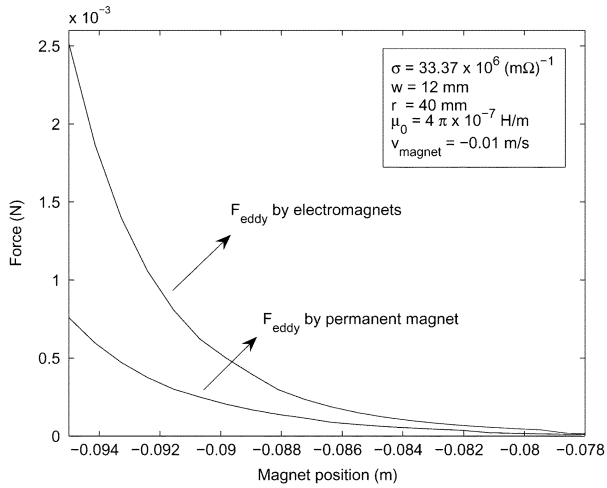

Fig. 6. Eddy forces formed by the permanent magnet and electromagnets. The plate is located at $z = -0.1$ m.

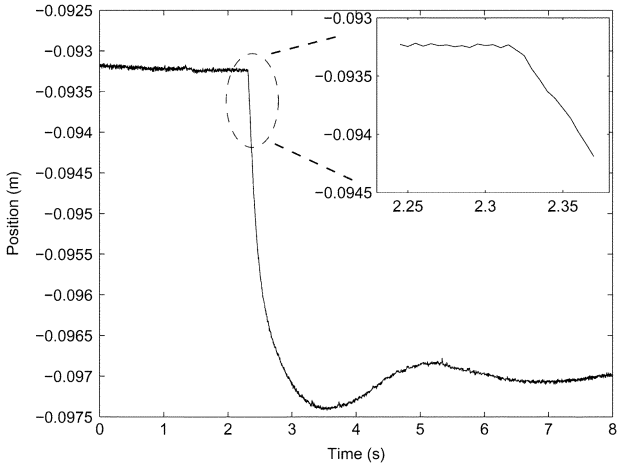

Fig. 7. Downward motion of the magnet. A 40 mm radius, 12 mm thick, Al-6061 plate is placed at $z = -0.1$ m.

the acceleration was calculated. To find the theoretical value of acceleration, $F_{\text{levitation}}$ is calculated by

$$F_{\text{levitation}} = \alpha I z + \beta I \tag{33}$$

where $\alpha = 0.9$ and $\beta = 0.12$ are experimental fitting constants. Equation (33) was obtained by curve fitting of experimental measurements. The procedure to obtain the levitation force formed by a magnetic drive unit with two electromagnets and a pole piece was explained in a previous study [24]. F_{eddy} was calculated numerically by (23). Acceleration was assumed to be constant during 5 ms intervals, so levitation and eddy forces were calculated at every 5 ms only.

Using the formula $\sum F = ma$, acceleration was calculated for the case with plate

$$F_{\text{levitation}} + F_{\text{eddy}} - mg = ma \tag{34}$$

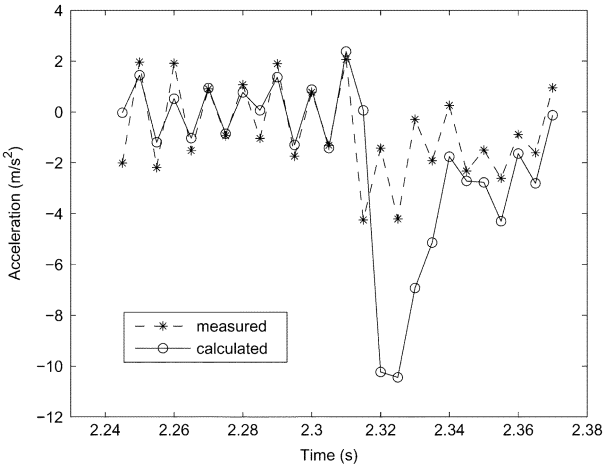

Fig. 8. Acceleration of the magnet. A 40 mm radius, 12 mm thick, Al-6061 plate is placed at $z = -0.1$ m.

where m is the mass of the object and g is the gravity constant. Fig. 8 illustrates the calculated and measured values. The calculated values match the experimental data except the beginning of the downfall. The discrepancy is mainly because of the rough approximation that acceleration remains constant during 5 ms. The decrease in the error during the fall (after 2.32 s) verifies this because when acceleration gets smaller in magnitude, the constant acceleration assumption becomes more valid. The other source of error is the hardware noise caused by the laser sensor, current amplifier and A-D converters. It was observed that F_{eddy} generated by the plate decreases the negative acceleration and slowed down the fall of the magnet. If the plate is removed, i.e., F_{eddy} is taken as zero in (34), acceleration increases in negative direction.

To verify the effect of eddy-current damping, we conducted experiments with different aluminum plates (Fig. 9). Plates only differ with their thicknesses: 9, 5, and 1 mm. They have a radius of 20 mm and an electrical conductivity of $33.37 \times 10^6\ (\text{m}\Omega)^{-1}$ at room temperature. They were located 0.1 m below the electromagnets. In all experiments the same trajectory (shown as dashed line) was given to the object to follow in a range of 30 mm.

It was observed that eddy currents achieve two tasks. First, minimizing the vibrations that were mainly caused by the inherent underdamped nature of the system. Secondly, guaranteeing a stable positioning for step inputs. For the plate with 9 mm of thickness, the levitated object could follow the step inputs and vibrations were damped to a level that cannot be detected by the naked eye. When the plate with thickness of 5 mm was used, the total value of eddy current decreased because of smaller thickness. Therefore, some vibrations were observed although the object followed the reference input. With the thinnest plate (1 mm), eddy-current force was almost nonexistent and control of the object could not be achieved for such a high-amplitude step input. At $t = 4$ s, the object fell onto the plate that is located at $z = -0.1$ m (Fig. 9(c)). At $t = 7$ s, the observer raised the object to the desired position by hand. The object followed the reference position with large fluctuations until $t = 14$ s when the next step input was applied.

Placing a 9 mm thick plate induced sufficient eddy currents (as Fig. 4 implies) that significantly reduced the vibrations.

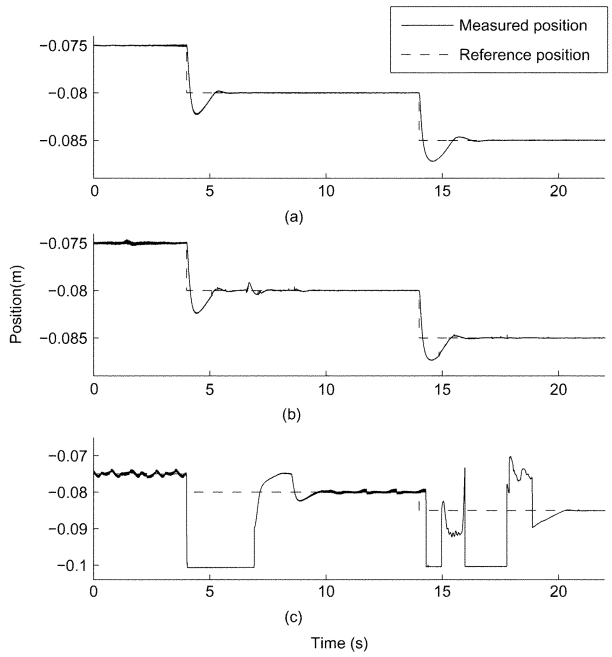

Fig. 9. Effect of plate thickness on eddy-current damping. Levitation with (a) 9-mm-thick plate, (b) 5-mm-thick plate, and (c) 1-mm-thick plate.

Also, with a closer look at Fig. 9(b) it can be realized that higher damping was achieved for $z = -0.085$ m compared to $z = -0.08$ and $z = -0.075$ m. Since eddy currents were larger when magnet was closer to the plate, lower vibrations were observed at $z = -0.085$ m. For a quantitative discussion, we plotted the position of the object (Fig. 10) for three different object heights when damping is formed by a 9 mm thick plate. These plots are enlarged portions of Fig. 9(a). Fig. 10 illustrates the fluctuations around the reference position during magnetic levitation. Table I summarizes the maximum and rms errors of position calculated for Fig. 10(a)–(c). As the derived F_{eddy} formula implies, when the plate was placed closer to the moving range, larger eddy force was generated (Fig. 6) resulting in a higher damping of vibrations. This allowed for a maximum steady-state precision of 39.14 μm when the object was levitated 15 mm above the plate. To further reduce this error, hardware noise, which is around 16 μm, should be reduced by higher resolution position measurement.

VI. Conclusion

In this paper, eddy-current damping was proposed to improve precision and stability of magnetic levitation. In order to calculate eddy-current force, a method based on a coil representation model was described. In the simplified model, vector magnetic potential was derived for any point in space. Then eddy-current density and magnetic field generated by induced eddy currents were calculated for corresponding regions. For the described magnetic levitation setup, representing the change in magnetic field with equivalent coils, the eddy-current force applied to a levitating object was obtained. The experiments verified that by placing a conductive plate underneath the levitated object, the excessive portion of levitation force that caused vibrations were effectively dissipated. The disturbance rejection of the system was enhanced resulting in a maximum static precision of 39.14 μm in a potential traveling range of 30 mm. It

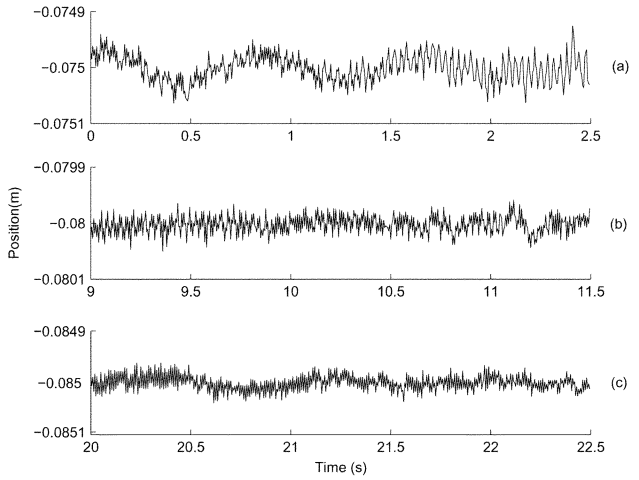

Fig. 10. Effect of plate-object distance on eddy-current damping. Levitation with a plate-object distance of (a) 0.025 m, (b) 0.020 m, and (c) 0.015 m.

TABLE I
POSITION ERROR FOR DIFFERENT PLATE-OBJECT DISTANCES

	(a)	(b)	(c)
Object height (m)	-0.075	-0.08	-0.085
Plate distance (m)	0.025	0.02	0.015
RMS error (μm)	23.99	17.38	16.08
Maximum error (μm)	74.26	50.13	39.14

can be foreseen that if the object is required to move in a smaller range, a higher precision can be achieved by placing the conductive plate much closer to the object. In addition, induced eddy currents ensure the stability of levitation for step transient motions by reducing acceleration of the object and synchronizing the motion with the controller. It was illustrated that eddy-current damping significantly improves the levitation performance without changing the controller algorithm or increasing the cost or complexity of the system enabling the set-up a potential tool for micromanipulation and micropositioning purposes.

REFERENCES

[1] C. E. Lin and H. L. Jou, "Model attitude control for magnetic suspension wind tunnel," *Proc. Nat. Sci. Council, Republic of China, Part A (Physical Science and Engineering)*, vol. 21, pp. 222–232, May 1997.

[2] S. E. Salcudean, N. M. Wong, and R. L. Hollis, "Design and control of a force-reflecting teleoperation system with magnetically levitated master and wrist," *IEEE J. Robot. Autom.*, vol. 11, pp. 844–858, Dec. 1995.

[3] F. N. Koumboulis and M. G. Skarpetis, "Static controllers for magnetic suspension and balance systems," *IEE Proc., Control Theory Appl.*, vol. 143, pp. 338–348, Jul. 1996.

[4] M. Komori and C. Shiraishi, "A levitated motor with superconducting magnetic bearings assisted by self-sensing AMB s," *IEEE Trans. Appl. Supercond.*, vol. 13, pp. 2189–2192, Jun. 2003.

[5] S. C. Mukhopadhyay, J. Donaldson, G. Sengupta, S. Yamada, C. Chakraborty, and D. Kacprzak, "Fabrication of a repulsive-type magnetic bearing using a novel arrangement of permanent magnets for vertical-rotor suspension," *IEEE Trans. Magn.*, vol. 39, pp. 3220–3222, Sep. 2003.

[6] T. Ohji, S. Ichiyama, K. Amei, M. Sakui, and S. Yamada, "Conveyance test by oscillation and rotation to a permanent magnet repulsive-type conveyor," *IEEE Trans. Magn.*, vol. 40, no. 4, pp. 3057–3059, Jul. 2004.

[7] S. Verma, W. J. Kim, and J. Gu, "Six-axis nanopositioning device with precision magnetic levitation technology," *IEEE/ASME Trans. Mechatron.*, vol. 9, pp. 384—391, , Jun. 2004.

[8] X. Y. Ye, Y. Huand, Z. Y. Zhou, Q. C. Li, and Q. L. Gong, "A magnetic levitation actuator for micro-assembly," in *Proc. IEEE Int. Conf. Solid-State Sensors and Actuators (Transducers'97)*, Chicago, IL, Jun. 1997, pp. 797–799.

[9] K. H. Park, K. Y. Ahn, S. H. Kim, and Y. K. Kwak, "Wafer distribution system for a clean room using a novel magnetic suspension technique," *IEEE/ASME Trans. Mechatron.*, vol. 3, pp. 73–78, Mar. 1998.

[10] M. Motokawa, M. Hamai, T. Sato, I. Mogi, S. Awaji, K. Watanabe, N. Kitamura, and M. Makihara, "Crsytal growth and materials processing in the magnetic levitation condition," *J. Magn. Magn. Mater.*, vol. 226–230, pp. 2090–2093, May 2001.

[11] M. Holmes, R. Hocken, and D. Trumper, "The long-range scanning stage: A novel platform for scanned-probe microscopy," *J. Int. Soc. Precision Eng. Nanotechnol.*, vol. 24, pp. 191–209, Jun. 2000.

[12] T. Nakamura and M. B. Khamesee, "A prototype mechanism for three-dimensional levitated movement of a small magnet," *IEEE/ASME Trans. Mechatron.*, vol. 2, pp. 41–50, Mar. 1997.

[13] M. B. Khamesee, N. Kato, Y. Nomura, and T. Nakamura, "Design and control of a microrobotic system using magnetic levitation," *IEEE/ASME Trans. Mechatron.*, vol. 7, pp. 1–14, Mar. 2002.

[14] H. A. Sodano and J. S. Bae, "Eddy current damping in structures," *Shock Vib. Dig.*, vol. 36, pp. 469–478, Nov. 2004.

[15] R. E. Cunningham, Passive eddy current damping as a means of vibration control in cryogenic turbomachinery NASA, Cleveland, OH, Tech. Rep. NASA-TP-2562, Jun. 1986.

[16] J. R. Fredrick and M. S. Darlow, "Operation of an electromagnetic eddy current damper with a supercritical shaft," *ASME J. Vib. Acoust.*, vol. 116, pp. 578–580, 1994.

[17] G. A. Haines and C. T. Leondes, "Eddy current nutation dampers for dual-spin satellites," *J. Astronaut. Sci.*, vol. 21, pp. 1–25, Aug. 1973.

[18] D. A. Kienholz, S. C. Pendleton, K. E. Richards, and D. R. Morgenthaler, "Demonstration of solar array vibration suppression [using eddy current dashpots]," in *Proc. SPIE—The International Society for Optical Engineering (Smart Structures and Materials '94)*, Orlando, FL, Feb. 1994, pp. 59–72.

[19] T. Yamaguchi, Y. Kawawse, H. Kodama, K. Hirata, Y. Hasegawa, and T. Ota, "Eddy current damping analysis of laser marker using 3-D finite element method," *IEEE Trans. Magn.*, vol. 42, no. 4, pp. 1011–1014, Apr. 2006.

[20] M. Schmid and P. Varga, "Analysis of vibration-isolating systems for scanning tunneling microscopes," *Ultramicroscopy*, vol. 42–44, pp. 1610–1615, July 1992.

[21] H. Teshima, M. Tanaka, K. Miyamoto, K. Noghuchi, and K. Hinata, "Effect of eddy current dampers on the vibrational properties in superconducting levitation using melt-processed ybacuo bulk superconductors," *Physica C*, vol. 274, pp. 17–23, Sept. 1997.

[22] C. S. Antonopoulos and E. E. Kriezis, "Force on a parallel circular loop moving above a conducting slab and the eddy-current distribution," *IEE Proc. A (Physical Science, Measurement and Instrumentation, Management and Education, Reviews)*, vol. 133, pp. 601–605, Dec. 1986.

[23] J. A. Tegopoulos and E. E. Kriezis, *Eddy Currents in Linear Conducting Media*. Amsterdam, The Netherlands: Elsevier, 1985.

[24] D. G. Craig and M. B. Khamesee, "Derivation of an analytical model for the force produced during the motion of a magnetically suspended object," in *Proc. IEEE Int. Conf. Mechatronics and Automation*, Niagara Falls, Canada, Jul. 2005, pp. 970–974.

Manuscript received February 14, 2006; revised October 4, 2006. Corresponding author: M. B. Khamesee (e-mail: khamesee@uwaterloo.ca).